

Analytical Methods

How to cite: *Angew. Chem. Int. Ed.* **2024**, *63*, e202314818
doi.org/10.1002/anie.202314818

Enzyme-Linked DNA Displacement (ELIDIS) Assay for Ultrasensitive Electrochemical Detection of Antibodies**

Ana Díaz-Fernández, Simona Ranallo,* and Francesco Ricci*

Abstract: Here we report the development of a method for the electrochemical ultrasensitive detection of antibodies that couples the programmability and versatility of DNA-based systems with the sensitivity provided by enzymatic amplification. The platform, termed Enzyme-Linked DNA Displacement (ELIDIS), is based on the use of antigen-DNA conjugates that, upon the bivalent binding of a specific target antibody, induce the release of an enzyme-DNA hybrid strand from a preformed duplex. Such enzyme-DNA hybrid strand can then be electrochemically detected with a disposable electrode with high sensitivity. We applied ELIDIS to demonstrate the sensitive (limit of detection in the picomolar range), specific and multiplexed detection of five different antibodies including three clinically relevant ones. ELIDIS is also rapid (it only requires two reaction steps), works well in complex media (serum) and is cost-effective. A direct comparison with a commercial ELISA kit for the detection of Cetuximab demonstrates the promising features of ELIDIS as a point-of-care platform for antibodies detection.

Introduction

Detection of IgG and IgM antibodies plays a critical role in the diagnosis of a variety of human diseases, providing information not only about current and past infection but also about disease progression and clinical outcomes.^[1,2] Antibodies are also gaining importance as therapeutics for autoimmune diseases and cancer. Their detection and monitoring can thus inform on therapy efficacy and dose optimization.^[3,4] Due to the low concentration (low nM to pM) at which antibodies are commonly found in clinical samples,^[5,6] methods for antibody detection must be not only

specific and selective but also highly sensitive.^[7,8] The enzyme-linked immunosorbent assay (ELISA), probably the most widely used approach for antibody detection,^[9] uses enzymatic amplification as a way to achieve very low limits of detection.^[10] However, this approach has the disadvantage of requiring reagent-intensive processes and multiple wash and reaction steps^[11] which result in relatively high costs and limit the applicability of this method at the point of care.^[12,13] Radioimmunoassay (RIA), another highly sensitive method for antibody detection, uses radioactively labelled antigens to provide information on antigen/antibody binding. However, this approach is also not without limitation as it requires the use and disposal of radioactive material, has cross-reactivity with matrix components and inter-batch variability.^[14]

In an effort to develop analytical platforms for antibody detection that are suitable for the point of care, we and other research groups have recently demonstrated several approaches that take advantage of the programmability and versatility of synthetic DNA to build nanoscale antibody-responsive devices.^[15-22] In these systems, synthetic DNA strands are used as molecular scaffolds to conjugate recognition elements (i.e. antigens) and signaling tags and are rationally designed to provide a signal when the target antibody binds to the antigens.^[23] In the last 10 years, several sensors using antigen-conjugated DNA strands and different sensing strategies (such as binding-induced conformational change, co-localization and steric hindrance) have been described.^[24-27] The advantages of such DNA-based systems include their great versatility and programmability. Indeed, by simply changing the recognition elements conjugated to the synthetic DNA strands, it is possible to recognize, in principle, any target antibody. Also, the programmability of DNA-DNA interactions along with the ability to use different orthogonal signal labels (both fluorescent and electrochemical) allows multiplexed detection of different antibodies in the same solution.^[28-31] These detection platforms are also characterized by high specificity, fast response time and low-cost. Despite the above advantages, however, all these approaches based on the use of antigen-conjugated DNA strands share a common limitation: due to the direct nature of the assays and the inherent instrumental limitations, the lowest antibody concentrations (limit of detection) that can be measured by these approaches is inevitably higher than those obtained by other indirect techniques such as ELISA. This important limitation ultimately impacts the potential use of these DNA-based platforms as point-of-care devices.

[*] A. Díaz-Fernández, S. Ranallo, F. Ricci
Department of Chemistry, University of Rome, Tor Vergata
Via della Ricerca Scientifica, 00133 Rome (Italy)
E-mail: simona.ranallo@uniroma2.it
francesco.ricci@uniroma2.it

A. Díaz-Fernández
Departamento de Química Física y Analítica, Universidad de Oviedo
Julián Clavería 8, 33006 Oviedo (Spain)

[**] A previous version of this manuscript has been deposited on a preprint server (10.26434/chemrxiv-2023-ncq8c-v2).

In response to the above considerations, we propose here a two-step assay, termed Enzyme-Linked DNA Displacement (ELIDIS) assay, that combines the programmability and versatility of antibody-responsive DNA-based systems with the sensitivity of enzyme amplification (Figure 1). In the first step (antibody-responsive reaction) we use antigen-conjugated DNA strands that induce the release of an enzyme-DNA hybrid strand from a preformed duplex complex upon the recognition of a specific target antibody (Figure 1, top). In the second step (amplification reaction), the reaction solution is transferred to an electrode surface so that the enzyme-DNA hybrid output strand can hybridize with a complementary strand immobilized on the electrode surface and provide a measurable current signal in the presence of the enzymatic substrate (Figure 1, bottom). We demonstrate here that this approach enables ultrasensitive detection of multiple antibodies in a rapid and specific manner.

Results and Discussion

To optimize the ELIDIS assay described above, we first characterized the two reaction steps separately. For the amplification step, we first selected Glucose Oxidase (GOx) as enzyme to be conjugated to the DNA output strand. We chose GOx because of its stability, high turnover rate and its wide use in electrochemical biosensor technology.^[32] For conjugation, we used a 30-nt DNA strand modified with dibenzocyclooctin (DBCO), which can be covalently con-

jugated to GOx via a crosslinker with a primary amine-reactive NHS group (Figure 2a). After the conjugation reaction, we purified the enzyme-DNA hybrid by ion exchange chromatography (Figure 2a, Figure S1). We then characterized the enzymatic amplification reaction by electrochemical measurements. For this purpose, we added increasing concentrations (from 10^{-15} to 10^{-6} M) of the GOx-DNA hybrid conjugate to a gold screen-printed disposable electrode modified with a complementary capture strand (Figure 2b). After an incubation step, we added glucose (200 mM) and measured the H_2O_2 produced using chronoamperometry (Figure 2c). We observed a concentration-dependent increase in the measured current with a $K_{1/2}$ (defined here as the GOx-DNA hybrid concentration at which the observed signal change is half of the maximum change) of $1.2 \pm 0.3 \times 10^{-12}$ M (Figure 2d). Control experiments, using electrodes modified with a non-specific capture strand or with mercaptohexanol alone produced a signal indistinguishable from the background signal even at saturating concentrations of the GOx-DNA hybrid strand (10^{-7} M) (see red and green dots respectively in Figure 2d).

Next, we proceeded to characterize the antibody-responsive reaction (step 1 in Figure 1). In this case, the reaction is based on the antibody-induced hybridization

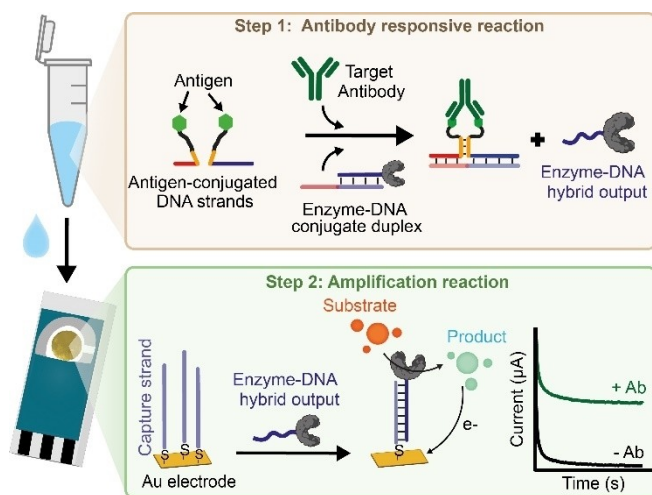


Figure 1. Scheme of the two reaction steps of ELIDIS assay. Step 1: Antibody-responsive reaction. The reaction employs two antigen-conjugated DNA strands that hybridize only in the presence of a target antibody. The formed complex is able to induce a strand displacement reaction that releases an enzyme-DNA hybrid strand from a pre-hybridized duplex. Step 2: Amplification reaction. The reaction solution of step 1 is transferred to the surface of a gold screen printed disposable electrode modified with a DNA capture strand complementary to the enzyme-DNA hybrid strand. After hybridization and addition of the substrate, the product generated by the enzymatic reaction is measured using chronoamperometry.

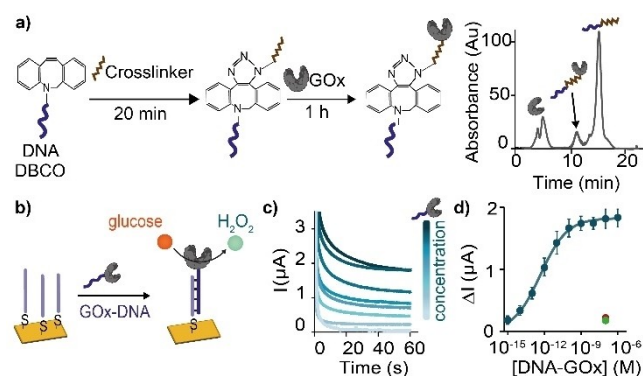


Figure 2. Characterization of the amplification reaction. a) Conjugation of Glucose Oxidase (GOx) to a DBCO-DNA strand and ion-exchange chromatography showing purification of the conjugate (see also Figure S1 for identification of the peaks). b) Schematic of electrochemical detection of the GOx-DNA hybrid strand. c) Chronoamperograms at different concentrations of the GOx-DNA hybrid strand. d) Plot showing the difference between the current signals obtained in the presence and absence of GOx-DNA hybrid strand vs. concentration of the GOx-DNA hybrid strand. Signals from control experiments using an electrode without a capture strand (red dot) and with a non-specific capture strand (green dot) are also shown. Details of the conjugation reaction can be found in the experimental section. Amplification reaction experiments were performed by adding a 10 μ L solution (150 mM NaCl, 50 mM NaH_2PO_4 , pH 7.0) containing different concentrations of the GOx-DNA hybrid strand on the surface of the working electrode. After 30 minutes of incubation at 25 $^{\circ}C$ the electrodes were washed and 50 μ L of glucose (200 mM) was added to the electrode surface. After 10 minutes a potential of 0.6 V was applied, and the current was measured continuously for 60 s. The signal for each concentration corresponds to the average intensity of the last 10 s of the measurement. The experimental values and error bars in this and the following figures represent the average and standard deviation of three independent measurements with three different electrodes.

between two antigen-conjugated DNA strands. The formed complex is capable of triggering a strand displacement reaction that releases the GOx-DNA hybrid strand from a preformed duplex. To optimize this step, it is crucial to find the optimal conditions under which hybridization between the two antigen-conjugated DNA strands occurs only upon bivalent binding of the target antibody. To this end, we first used the small molecule digoxigenin (Dig) and the antibody anti-Dig as antigen and target antibody, respectively (Figure 3a). We then synthesized a series of Dig-conjugated DNA strands with complementary domains of different lengths. We tested lengths from 0 to 14 bases corresponding to estimated values of hybridization free energy from 0 to $-23 \text{ kcal mol}^{-1}$, respectively. For each set of Dig-conjugated strands, we performed the reaction in the absence and presence of a fixed concentration of anti-Dig antibody (10^{-8} M) and measured the electrochemical signal generated by the GOx-DNA output strand on a disposable electrode as described previously (Figure 3b). As expected, Dig-conjugated strands with short complementary portions (< 4 nucleotides) yield low signals in both the absence and presence of anti-Dig antibody. With longer complementary portions (> 8 nucleotides) we observe higher background signals as the two antigen-conjugated strands tend to hybridize spontaneously even in the absence of the target antibody. A complementary domain of 6 nucleotides provides the highest signal change in the presence of the antibody and was therefore selected for future experiments. Using these Dig-conjugated DNA strands and previously described amplification step, we tested increasing concentrations (from 10^{-15} to 10^{-6} M) of anti-Dig antibody. In this way, we obtained a dose-response curve with a dynamic range (defined as the concentration range in which we obtain signals between 10 % and 90 % of the maximum signal) between 3×10^{-13} and $3 \times 10^{-11} \text{ M}$ of anti-Dig antibody with a detection limit (LOD) (defined as the concentration that reaches a signal three standard deviations above a blank) of $1 \times 10^{-12} \text{ M}$ and an average RSD % of 11 % (Figure 3c,d). The observed current saturation signal in these conditions is smaller compared to that obtained from direct hybridization of the GOx-DNA strand (see Figure 2c–d, Figure S2). This difference is likely due to the fact that the antibody-responsive reaction is not 100 % efficient as the same target antibody can bind to two antigen-conjugated strands thus not providing any signal. ELIDIS works well also in complex media. To demonstrate this, we performed the reaction step (step 1) in 80 % bovine serum and we obtained similar results in terms of dynamic range (between 4×10^{-13} and $2 \times 10^{-11} \text{ M}$), $K_{1/2}$ ($3 \pm 1 \times 10^{-12} \text{ M}$), LOD ($1 \times 10^{-12} \text{ M}$). We note here that a recently reported antibody-responsive strand displacement reaction coupled with electrochemical detection without an enzymatic amplification (the output strand binds to a redox-reporter modified complementary strand immobilized on a disposable electrode) provides poorer sensitivity (LOD in the nM range) and requires longer assay time^[29] thus demonstrating the crucial role of the enzymatic amplification step to achieve the high sensitivity displayed by ELIDIS.

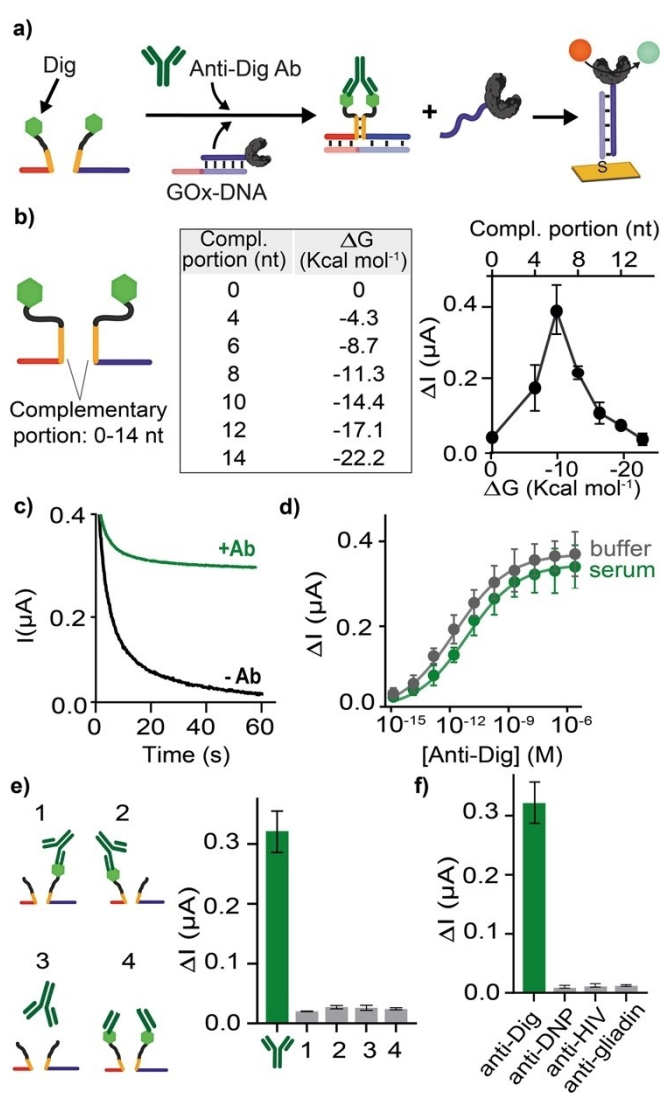


Figure 3. Optimization of the antibody-responsive reaction. a) Schematic of anti-Dig responsive strand displacement reaction. b) Differences in current signals obtained in the presence and absence of anti-Dig antibodies using Dig-conjugated DNA strands with variable length of complementary portions (estimated hybridization free energy values using *mfold* web server at 25 °C, $[\text{Na}^+] = 0.15 \text{ M}$ and $[\text{Dig-conjugated strand}] = 160 \text{ nM}$ is also shown). c) Chronoamperograms obtained in the absence and presence of anti-Dig antibodies (10 nM) using Dig-conjugated DNA strands with 6-nt complementary portions. d) Current vs anti-Dig antibodies concentration in buffer solution and serum (80%). e) Current values obtained at saturating concentration (100 nM) of anti-Dig antibodies and anti-Dig Fab Fragment for different control experiments. f) Current values obtained at saturating concentration (100 nM) of anti-Dig antibodies and other non-specific antibodies. The reaction was performed at 25 °C in a $10 \mu\text{L}$ buffer solution (150 mM NaCl , $50 \text{ mM NaH}_2\text{PO}_4$, pH 7.0) or 80% of bovine serum containing the pre-hybridized DNA duplex (100 nM), the antigen-conjugated DNA strands (160 nM each) and the Anti-Dig antibody. After 30 minutes the solution was transferred to the electrode surface for the amplification reaction (see legend of Figure 2 for the experimental conditions of this step).

The platform is also highly specific: we did not observe any measurable signal in control experiments using only one

Dig-conjugated DNA strand (#1 and #2, Figure 3e) or both strands unconjugated (#3, Figure 3e). We also observed no signal using anti-Dig Fab fragments (instead of intact anti-Dig antibodies), which was expected due to the monovalent nature of the Fab fragments (#4, Figure 3e). Furthermore, when we added saturating concentrations of non-specific antibodies, we recorded signals that were indistinguishable from background (Figure 3f).

ELIDIS is easily adaptable to the detection of different target antibodies by simply changing the recognition element conjugated to the DNA strands. To demonstrate this, we engineered an antibody-responsive DNA strand displacement reaction for the detection of anti-DNP antibodies (Figure S3a). This platform showed concentration-dependent current signals (Figure S3b) that allowed detection of anti-DNP antibodies in 80 % bovine serum with a dynamic range (between 3×10^{-13} and 2×10^{-11} M), sensitivity ($K_{1/2} = 3 \pm 1 \times 10^{-12}$ M; $\text{LOD} = 3 \times 10^{-12}$ M) (Figure S3c) and specificity (Figure S3d) comparable to those observed with anti-Dig antibodies.

ELIDIS can also be adapted to a modular version in which the antigen-conjugated strands hybridize with the DNA strands responsible for the strand displacement reaction (Figure 4a). This modular approach allows the use of more complex recognition elements (i.e., peptide epitopes, proteins, etc.). For example, using this modular version of ELIDIS, we measured two different monoclonal antibodies directly in serum: the anti-MUC (Figure 4b) antibody and Cetuximab (Figure 4c). For anti-MUC antibody, we used as antigen a peptide (15 amino acids) excised from the MUC1 protein (MUC peptide). For Cetuximab we used the entire EGFR protein as antigen. The same approach can also be used to detect a bispecific antibody (Figure 4d). In this case, we measured a bispecific antibody re-engineered to contain one binding site that binds the EGFR protein and the other that targets MUC1 protein. For this target antibody we then used two different antigen-conjugated strands conjugated to EGFR and the MUC peptide (Figure 4d, bottom). For all these modular ELIDIS platforms, we achieved sensitivities and specificities comparable to their non-modular counterpart, with LOD values in the picomolar range (i.e., $\text{LOD Anti-MUC Ab} = 2 \times 10^{-12}$ M; $\text{LOD Cetuximab} = 1 \times 10^{-12}$ M; $\text{LOD Bispecific Ab} = 4 \times 10^{-13}$ M) and average $\text{RSD}\% < 12\%$ (Figure 4).

For a better analytical characterization of the developed ELIDIS platform, we compared the analytical performance with that of a commercial ELISA kit. For this purpose, we selected the modular ELIDIS assay for the detection of Cetuximab. ELIDIS provides better sensitivity ($\text{LOD of the ELISA kit} = 6 \times 10^{-10}$ M) with fewer experimental steps and comparable overall assay time (Figure 5a–b, Table S1). We also examined the recoveries of spiked blank serum samples for different Cetuximab concentrations (from 10^{-12} to 10^{-7} M) using ELIDIS platform and the commercial ELISA assay (Figure 5c). We observe comparable recoveries between ELISA and ELIDIS in the concentration range between 10^{-8} and 10^{-7} M. It is noteworthy that the ELISA kit does not provide quantitative information below 10^{-9} M,

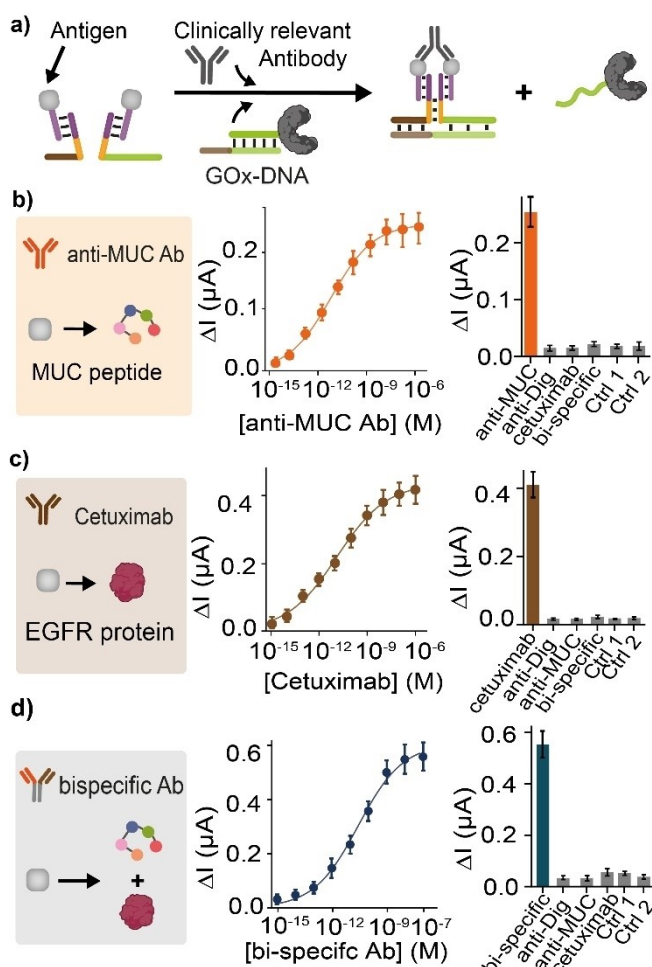


Figure 4. Ultrasensitive electrochemical detection of antibodies by the modular ELIDIS assay. a) General scheme of the modular ELIDIS assay. Panels b–d show the elements used (left), the dose-response curves (middle) and the specificity results (right) for the detection of anti-MUC antibody, c) Cetuximab and d) a bispecific antibody. Experiments were performed in a $10 \mu\text{L}$ solution containing 80% bovine serum and the pre-hybridized DNA duplex (100 nM), the antigen-DNA strands (160 nM each), and the elements for each antibody detection: MUC peptide-PNA (320 nM), EGFR-DNA (160 nM) or MUC peptide-PNA and EGFR-DNA for anti-MUC, Cetuximab and the bispecific antibody respectively. The DNA strands and the target antibody were allowed to react for 30 minutes at RT and then transferred to the disposable electrode for the amplification reaction (see legend of Figure 2 for experimental conditions of the amplification).

whereas ELIDIS remains sensitive even at a concentration of 10^{-12} M.

ELIDIS can be easily multiplexed and allows simultaneous detection of multiple antibodies in the same sample. To demonstrate this, we rationally designed two different antibody-responsive DNA strand displacement reactions (with different DNA sequences), each of which responding to a specific antibody (anti-Dig and Cetuximab). Thus, each reaction releases a specific GOx-DNA strand in the presence of the target antibody. We then used a disposable electrode that has the same reference and counter electrode but presents two different working electrodes, each modified

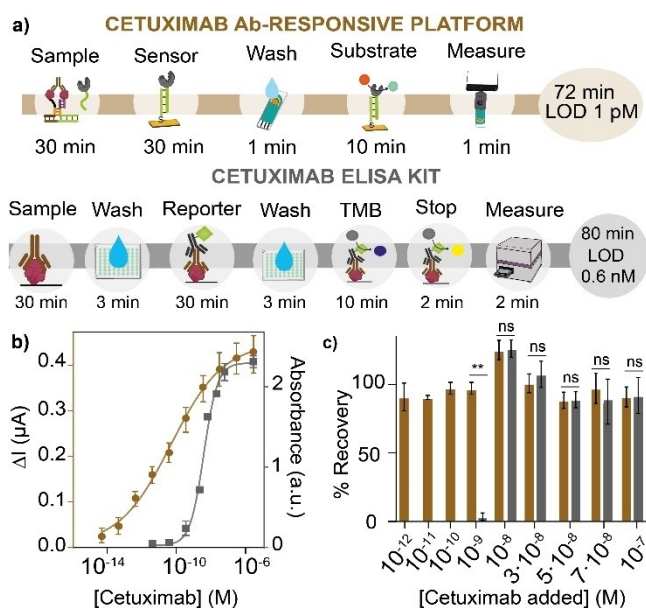


Figure 5. Comparison between ELIDIS and a commercial ELISA kit for the detection of Cetuximab. a) General scheme of the steps and time required for the two assays. b) Dose-response curves obtained with ELIDIS assay (brown) and the ELISA kit (grey). c) Recovery values of Cetuximab obtained by spiking blank serum samples with known concentrations of Cetuximab (from 10^{-12} to 10^{-7} M) determined using ELIDIS assay (brown) and the ELISA kit (grey). Experimental details of ELIDIS assay can be found in the legend of Figure 4. The ELISA kit was performed according to the manufacturer's instructions (see Supporting Information for details). Statistical analysis was performed with Prism GraphPad 9vs using two-tailed unpaired Student's *t* test, and the *p*-value ranges are indicated with black asterisks (** = 0.001–0.01, ns = non-significant).

with a capture probe specific for each GOx-DNA output strand. We mixed the two ELIDIS systems in the same tube and challenged them with different combinations of the two target antibodies and then transferred the solution to the electrode surface for measurement (Figure 6a). As expected, each sensor produced a measurable current signal for its specific antibody with minimal cross-reactivity (Figure 6b).

Conclusion

Here we have presented an electrochemical assay, termed ELIDIS, for ultrasensitive detection of specific antibodies that combines the programmability and versatility of antibody-responsive DNA-based devices with those of enzymatic amplification. More specifically, ELIDIS is a two-step assay that uses antigen-conjugated DNA strands and enzyme-DNA hybrids for the electrochemical detection of multiple target antibodies. The platform provides detection limits in the pM range, is specific (no signal is observed in the presence of non-targeted antibodies), and works well also in 80% of serum. A direct comparison with a commercial ELISA kit shows that ELIDIS is competitive in terms of sensitivity, assay time, cost, and simplicity of reaction steps (Scheme S1). It was not possible to directly

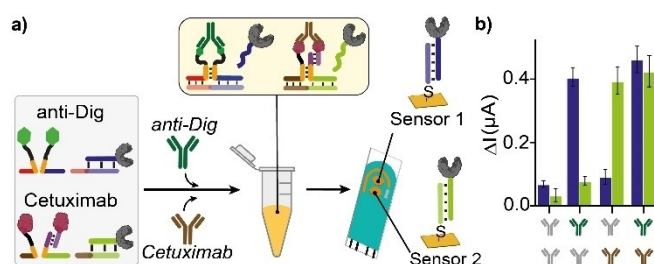


Figure 6. Dual detection of two different antibodies in the same sample using ELIDIS assay. a) Schematic of multiplex detection of anti-Dig antibodies and Cetuximab using two orthogonal antibody-induced DNA strand displacement reactions in the same sample. b) Current signals obtained with solutions containing different combinations of the two antibodies. Experiments were performed at 25 °C in a 20 μ L solution containing each of the GOx-DNA duplexes (100 nM each), the antigen-conjugated strands (160 nM each), the EGFR-DNA strand (180 nM) and the indicated antibodies (100 nM). After addition of the antibodies, the solution was allowed to react at 25 °C for 30 minutes and then transferred to the electrode surface for the amplification reaction (see legend of Figure 2 for experimental conditions of the amplification).

compare our approach with chemiluminescence assay (CLEIA) as no commercial kits were available for the same target antibodies we tested here. Despite this, considering the reported sensitivities for similar protein targets^[33,34] it is likely that CLEIA can provide a slightly better sensitivity than ELIDIS. ELIDIS is also versatile: we demonstrated detection of five different antibodies, including a bispecific antibody, by simply changing the recognition element conjugated to the DNA strand. Finally, the platform can be easily multiplexed by using different antibody-responsive reactions, with different DNA sequences rationally design employing computer-aided design^[35–37] and commercially available disposable electrodes modified with different capture strands. Thanks to the above properties, we believe that the use of modified synthetic DNA strands in combination with enzymatic amplification and electrochemical detection can open a new avenue for the development of highly sensitive platforms for antibody detection.

Supporting Information

Material and methods, sequences of nucleic acids and Figures can be found in the Supporting Information.

Acknowledgements

Ana Díaz-Fernández thanks Ministerio de Universidades of the Spanish Government for the postdoctoral Margarita Salas fellowship of the “Ayudas para la recualificación del sistema universitario español para 2021–2023”, financed by European Union-Next Generation EU.

Conflict of Interest

The authors declare no conflict of interest.

Data Availability Statement

The data that support the findings of this study are available from the corresponding author upon reasonable request.

Keywords: Antibody · DNA Nanotechnology · Electrochemical Biosensors · Enzymes · Synthetic Biology

-
- [1] J. T. Ballew, J. A. Murray, P. Collin, M. Mäki, M. F. Kagnoff, K. Kaukinen, P. S. Daugherty, *Proc. Natl. Acad. Sci. USA* **2013**, *110*, 19330–19335.
- [2] F. Krammer, V. Simon, *Science* **2020**, *368*, 1060–1061.
- [3] S. Zinn, R. Vazquez-Lombardi, C. Zimmermann, P. Sapra, L. Jermutus, D. Christ, *Nat. Cancer* **2023**, *4*, 165–180.
- [4] A. C. Chan, P. J. Carter, *Nat. Rev. Immunol.* **2010**, *10*, 301–316.
- [5] M. Leeman, J. Choi, S. Hansson, M. U. Storm, L. Nilsson, *Anal. Bioanal. Chem.* **2018**, *410*, 4867–4873.
- [6] F. Robert, M. P. Ezekiel, S. A. Spencer, R. F. Meredith, J. A. Bonner, M. B. Khazaeli, M. N. Saleh, D. Carey, A. F. Lobuglio, R. H. Wheeler, M. R. Cooper, H. W. Waksal, *J. Clin. Oncol.* **2001**, *19*, 3234–3243.
- [7] K. J. Land, D. I. Boeras, X. S. Chen, A. R. Ramsay, R. W. Peeling, *Nat. Microbiol.* **2019**, *4*, 46–54.
- [8] Y. Wu, R. D. Tilley, J. J. Gooding, *J. Am. Chem. Soc.* **2019**, *141*, 1162–1170.
- [9] R. M. Lequin, *Clin. Chem.* **2005**, *51*, 2415–2418.
- [10] H. Hayrapetyan, T. Tran, E. Tellez-Corrales, C. Madiraju, *ELISA Methods and Protocols* (R. S. Matson, R. S.), Springer US, New York, **2023**, pp. 1–17.
- [11] K. N. Baker, M. H. Rendall, A. Patel, P. Boyd, M. Hoare, R. B. Freedman, D. C. James, *Trends Biotechnol.* **2002**, *20*, 149–156.
- [12] N. Jiang, N. D. Tansukawat, L. Gonzalez-Macia, H. C. Ates, C. Dincer, F. Güder, S. Tasoglu, A. K. Yetisen, *ACS Sens.* **2021**, *6*, 2108–2124.
- [13] S. Nayak, N. R. Blumenfeld, T. Laksanasopin, S. K. Sia, *Anal. Chem.* **2017**, *89*, 102–123.
- [14] R. Liu, S. Zhang, C. Wei, Z. Xing, S. Zhang, X. Zhang, *Acc. Chem. Res.* **2016**, *49*, 775–783.
- [15] W. Engelen, L. H. H. Meijer, B. Somers, T. F. A. De Greef, M. Merkx, *Nat. Commun.* **2017**, *8*, 14473.
- [16] B. M. G. Janssen, M. Van Rosmalen, L. Van Beek, M. Merkx, *Angew. Chem. Int. Ed.* **2015**, *54*, 2530–2533.
- [17] S. Bracaglia, S. Ranallo, F. Ricci, *Angew. Chem. Int. Ed.* **2023**, *62*, e202216512.
- [18] S. Ranallo, C. Prévost-Tremblay, A. Idili, A. Vallée-Bélisle, F. Ricci, *Nat. Commun.* **2017**, *8*, 15150.
- [19] S. Ranallo, D. Sorrentino, F. Ricci, *Nat. Commun.* **2019**, *10*, 5509.
- [20] M. Rossetti, R. Ippodrino, B. Marini, G. Palleschi, A. Porchetta, *Anal. Chem.* **2018**, *90*, 8196–8201.
- [21] H. Zhang, F. Li, B. Dever, C. Wang, X. F. Li, X. C. Le, *Angew. Chem. Int. Ed.* **2013**, *52*, 10698–10705.
- [22] A. Idili, A. Bonini, C. Parolo, R. Alvarez-Diduk, F. Di Francesco, A. A. Merkoçi, *Adv. Funct. Mater.* **2022**, *32*, 2201881.
- [23] S. Ranallo, A. Porchetta, F. Ricci, *Anal. Chem.* **2019**, *91*, 44–59.
- [24] S. S. Mahshid, S. Camiré, F. Ricci, A. A. Vallée-Bélisle, *J. Am. Chem. Soc.* **2015**, *137*, 15596–15599.
- [25] A. Porchetta, R. Ippodrino, B. Marini, A. Caruso, F. Caccuri, F. Ricci, *J. Am. Chem. Soc.* **2018**, *140*, 947–953.
- [26] A. Desrosiers, A. Vallée-Bélisle, *Nanomedicine* **2017**, *12*, 175–179.
- [27] S. Ranallo, S. Bracaglia, D. Sorrentino, F. Ricci, *ACS Sens.* **2023**, *8*, 2415–2426.
- [28] J. Hu, Y. Yu, J. C. Brooks, L. A. Godwin, S. Somasundaram, F. Torabinejad, J. Kim, C. Shannon, C. J. A. Easley, *J. Am. Chem. Soc.* **2014**, *136*, 8467–8474.
- [29] S. Bracaglia, S. Ranallo, K. W. Plaxco, F. Ricci, *ACS Sens.* **2021**, *6*, 2442–2448.
- [30] A. Patino Diaz, S. Bracaglia, S. Ranallo, T. Patino, A. Porchetta, F. Ricci, *J. Am. Chem. Soc.* **2022**, *144*, 5820–5826.
- [31] C. T. Tsai, P. V. Robinson, C. A. Spencer, C. R. Bertozzi, *ACS Cent. Sci.* **2016**, *2*, 139–147.
- [32] S. B. Bankar, M. V. Bule, R. S. Singhal, L. Ananthanarayan, *Biotechnol. Adv.* **2009**, *27*, 489–501.
- [33] R. Tanaka, M. Takemura, M. Sato, Y. Yamada, T. Nakagawa, T. Horibe, M. Hoshi, H. Otaki, H. Ito, M. Seishima, K. Shimizu, *Clin. Chim. Acta* **2010**, *411*, 22–25.
- [34] M. S. Ashenagar, A. Matsumoto, H. Sakai, M. Tokiya, M. Hara, Y. Hirota, *Vaccine* **2022**, *10*, 487.
- [35] R. Owczarzy, A. V. Tataurov, Y. Wu, J. A. Manthey, K. A. McQuisten, H. G. Almabrazi, K. F. Pedersen, Y. Lin, J. Garretson, N. O. McEntaggart, C. A. Sailor, R. B. Dawson, A. S. Peek, *Nucleic Acids Res.* **2008**, *36*, W163–W169.
- [36] D. Mao, C. Lu, R. Zhang, L. Zhu, Y. Song, C. Feng, Q. Zhang, T. Chen, Y. Yang, G. Chen, X. Zhu, W. Tan, *Anal. Chem.* **2022**, *94*, 10263–10270.
- [37] J. N. Zadeh, C. D. Steenberg, J. S. Bois, B. R. Wolfe, M. B. Pierce, A. R. Khan, R. M. Dirks, N. A. Pierce, *J. Comput. Chem.* **2011**, *32*, 170–17.

Manuscript received: October 4, 2023

Accepted manuscript online: November 23, 2023

Version of record online: November 30, 2023